[?], [?], [?], [?], [?]. Nevertheless, there is an unmet need for a general mathematical framework allowing the analysis and design of cellular networks for both legacy ground users and UAV corridors. Stochastic geometry, a commonly used tool to analyze coverage and interference patterns for random spatial distributions of nodes (including UAVs [?], [?]) is not well-suited to optimize cellular networks for specific UAV corridors via deterministic BS deployments.

B. Contribution and Summary of Results

In this paper, we take the first step towards creating such mathematical framework through quantization theory, already proven successful in addressing problems that involve the geographical deployment of agents [?], [?], [?], [?], [?], [?], [?], [?], [?], [?], [?], [?]. Specifically, we determine the necessary conditions and design iterative algorithms to optimize the antenna tilts and transmit power at each BS of a cellular network to provide the best quality of service to both legacy ground users and UAVs flying along corridors. To the best of our knowledge, this is the first work doing so in a rigorous yet tractable manner, while accounting for a realistic network deployment, antenna radiation pattern, and propagation channel model.

We conduct a comprehensive mathematical analysis and develop optimization algorithms for three system-level performance metrics, each averaged across all users within the target region: (i) average received signal strength (RSS), which serves as a proxy for coverage; (ii) average SINR, which serves as a proxy for quality of service; and (iii) max-product SINR and soft-max-min SINR, which allow to trade quality of service for fairness among users through tunable hyperparameters. Our analysis accommodates a generic 3D user distribution, enabling prioritization of performance on the ground, along UAV corridors, or any desired tradeoff between the two.

To illustrate the effectiveness of our mathematical framework, we further present multiple case studies, whose main takeaways can be summarized as follows:

- As expected, optimizing the antenna tilts for average RSS, with a focus on ground users or UAV corridors, results in all BSs either being downtilted or uptilted, respectively. However, by pursuing a tradeoff between the ground and the sky, we achieve a non-trivial combination of uptilted and downtilted antennas. This arrangement involves a subset of BSs catering to UAV corridors while maintaining coverage on the ground.
- Optimizing the network for SINR leads to a subset of BSs operating at maximum power, while the remaining ones operate at lower power levels or are altogether deactivated. This arrangement aims to provide a sufficiently strong signal while mitigating intercell interference, especially along UAV corridors.
- Through the optimal combinations of antenna tilts and transmit power, which are non-obvious and otherwise difficult to design heuristically, our proposed algorithms significantly enhance coverage and signal quality along UAV corridors. These improvements are achieved with
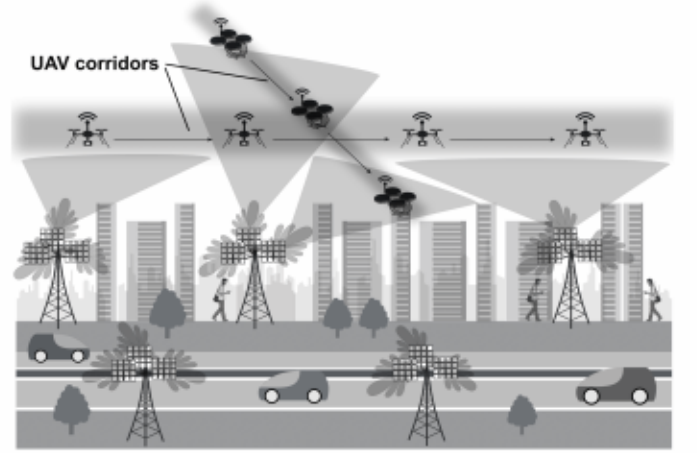

Fig. 1: Illustration of a cellular network with downtilted and uptilted BSs providing coverage to ground users as well as UAVs flying along corridors (blurred gray).

only a marginal reduction in ground performance compared to a scenario devoid of UAVs.

II. SYSTEM MODEL

The cellular network under consideration is depicted in Fig. ?? and detailed as follows.

A. Network Topology

1) Ground Cellular Network: The underlying infrastructure of our network is a terrestrial cellular deployment consisting of N BSs that provide service to network users. The height and 2D location of BS n is denoted by $h_{n,\mathrm{B}}$ and $\boldsymbol{p}_n$, respectively, for each $n \in \{1, \cdots, N\}$. Let $\boldsymbol{\Theta} = (\theta_1, \cdots, \theta_N)$ where $\theta_n \in [-90°, +90°]$ is the vertical antenna tilt of BS n, that can be adjusted by a mobile operator, with positive and negative angles denoting uptilts and downtilts, respectively. Let $\boldsymbol{\rho} = (\rho_1, \cdots, \rho_N)$ where ρ_n is the transmission power of BS n, measured in dBm, which is also adjustable by a mobile operator with a maximum value of $\rho_{\max}$. We denote the antenna horizontal boresight direction (azimuth) of BS n by $\phi_n \in [-180°, +180°]$ which is assumed to be fixed upon deployment.

2) UAV Corridors and Legacy Ground Users: There are two types of users being served by the BSs: (i) UAVs that traverse a region $Q_U = \bigcup_{u=1}^{N_U} Q_u$ consisting of N_U predefined 2D aerial routes/corridors Q_u; and (ii) ground-users (GUEs) that are dispersed over a 2D region Q_G. For each $1 \le u \le N_U$, all UAVs flying in the aerial corridor Q_u are assumed to have a fixed height h_u. In addition, we consider a fixed height h_G for all GUEs. Let $\lambda(\boldsymbol{q})$ be a probability density function that represents the distribution of users in the target region $Q = Q_U \bigcup Q_G$. Each user is associated with one BS; thus, the target region Q is partitioned into N disjoint subregions $\boldsymbol{V} = (V_1, \cdots, V_N)$ such that users within V_n are associated with BS n.

(a) GUEs, setup as per Sec. ??.
(b) GUEs, setup as per Section ?? ×2.
(c) GUEs, setup as per Section ?? ×4.
(d) UAVs, setup as per Section ??.
(e) UAVs, setup as per Section ?? ×2.
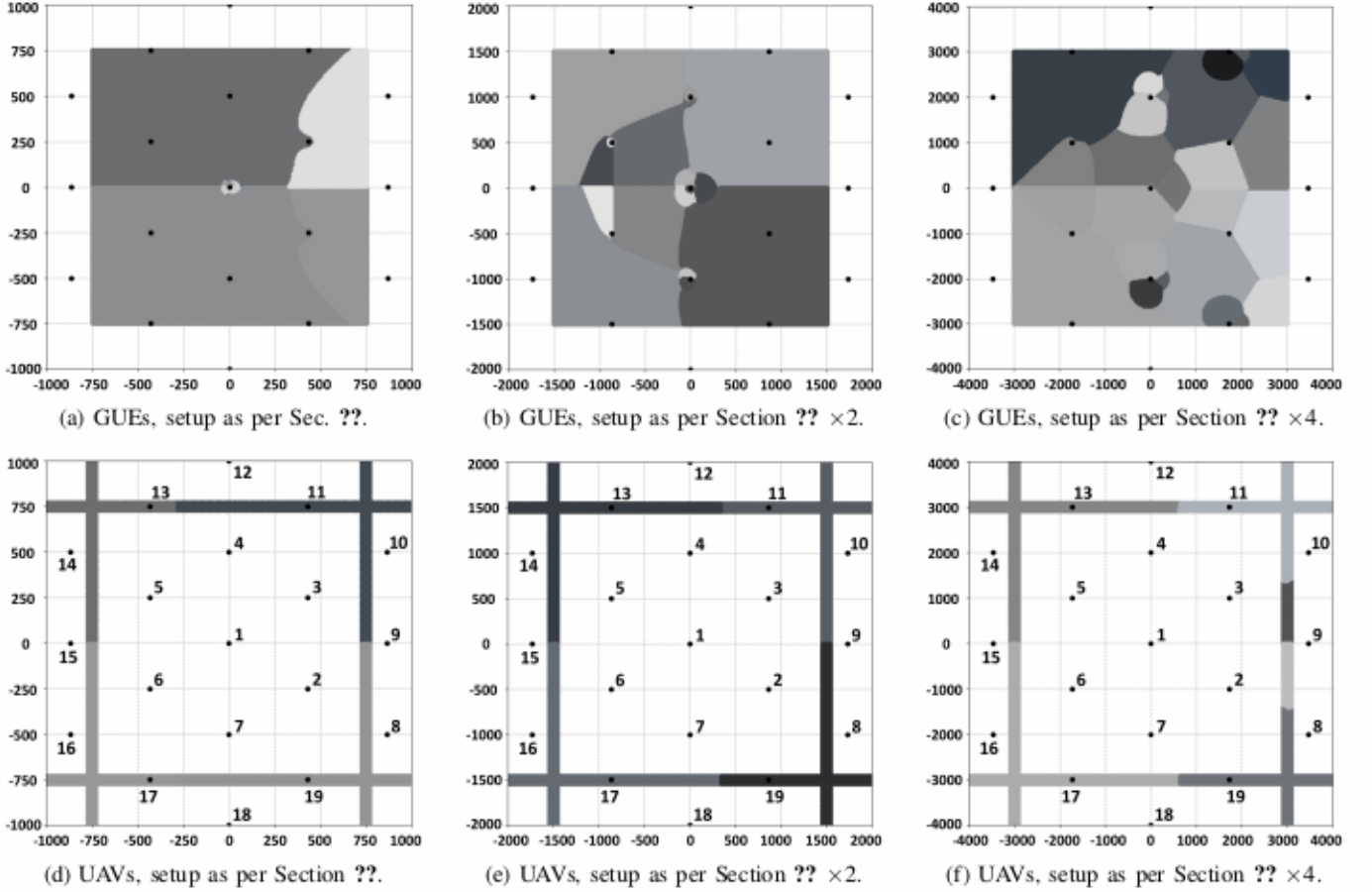(f) UAVs, setup as per Section ?? ×4.

Fig. 2: Optimized GUEs and UAVs cell partitioning for the Max-SINR-PA-VAT algorithm with $r = 0.5$. Simulations are carried out for three different target region sizes and BS intersite distances.

situation is exemplified in Fig. ??, where BSs that do not contribute to the performance function in any of the three simulated scenarios ($r = 0, 0.5$, and 1) are depicted as black squares.

2) Optimal Transmission Power: Figs. ?? and ?? present the optimal transmission power values, ρ_n^*, for the Max-SINR-PA-VAT and MP-PA-VAT algorithms. In each of the three scenarios, namely $r = 0$, $r = 0.5$, and $r = 1$, a subset of BSs operates at the maximum power level of $43\,\text{dBm}$, while another subset utilizes lower power levels, and the remaining BSs are deactivated. While not shown, similar observations are made for the SMM-PA-VAT algorithm. This is in contrast to the Max-RSS-VAT algorithm where all BSs are set to the optimal transmission power value of $43\,\text{dBm}$. However, as the target region and ISD grow larger, the impact of interference diminishes and more BSs become active. This is demonstrated in Fig. ?? where the Max-SINR-PA-VAT algorithm is utilized to determine the most favorable network configuration for three distinct combinations of GUE and UAV target region sizes and ISD values in the case of $r = 0.5$. The initial pair, depicted in Figs. ?? and ??, corresponds to the setup described in Section ??. For the second pair, showcased in Figs. ?? and ??, the GUE target region, distance between UAV corridors, and their respective widths, along with the BS ISD, are all doubled. Consequently, the optimal partitioning of the GUE

target region in Fig. ?? reveals an increased number of cells and more active BSs. Finally, expanding the setup in Figs. ?? and ?? by an additional factor of two yields the configuration depicted in Figs. ?? and ??. The second expansion results in a further increase in the number of cells for both the optimal GUE and UAV target region partitioning. This is primarily due to the reduced impact of interference at larger distances, allowing more BSs to efficiently serve users in their vicinity.

3) Performance Improvement: Fig. ?? shows the cumulative distribution function (CDF) of the RSS perceived by ground users (solid line) and UAVs (dash-dash line) when the antenna tilts are optimized through the Max-RSS-VAT algorithm for ground users only ($r = 1$, green), UAVs only ($r = 0$, blue), and both ($r = 0.5$, red). Note that the ground user performance for $r = 1$ (green solid line) and the UAV performance for $r = 0$ (blue dash-dash line) can be regarded as respective upper bounds (in mean) since they entail optimizing all vertical tilts for ground users only and for UAVs only, respectively. Conversely, the ground user performance for $r = 0$ (blue solid line) and the UAV performance for $r = 1$ (green dash-dash line) can be regarded as respective baselines obtained when the vertical tilts are chosen ignoring ground users and UAVs, respectively. Fig. ?? shows that for $r = 0.5$ the proposed Max-RSS-VAT algorithm reaches a satisfactory tradeoff by: (i) significantly
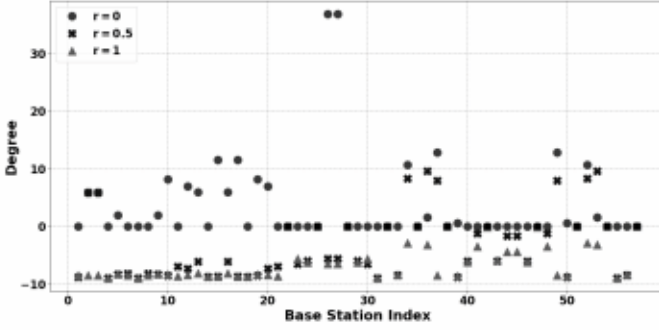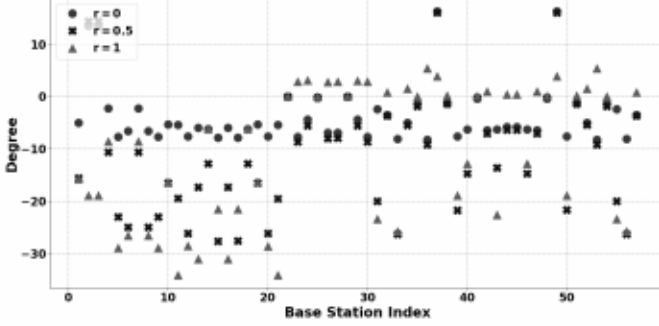
(a) Max-RSS-VAT algorithm.
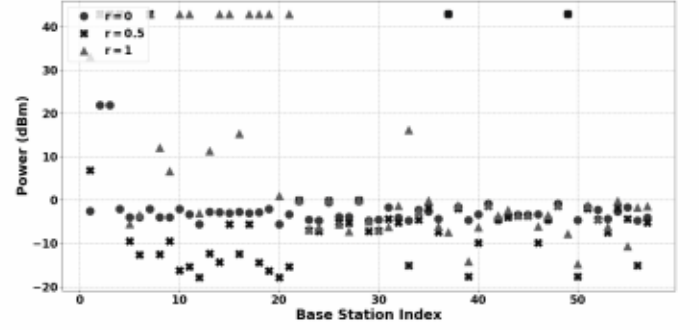

(b) MP-PA-VAT algorithm with $\mu = \nu = 0.1$.

Fig. 3: Optimized vertical tilts, θ_i^*: (a) Max-RSS-VAT and (b) MP-PA-VAT Algorithm with $\mu = \nu = 0.1$. Optimized for: GUEs only (green triangles, $r = 1$), UAVs only (blue circles, $r = 0$), and both GUEs and UAVs (red crosses, $r = 0.5$).
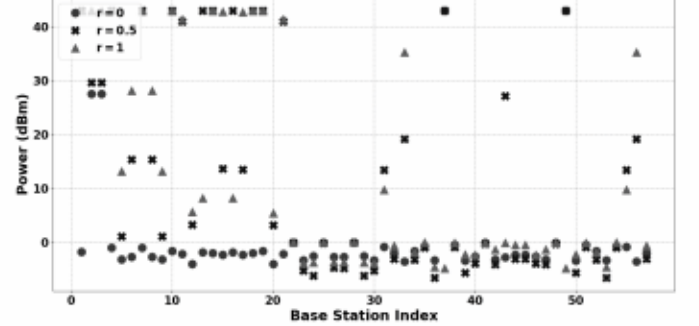

(a) Max-SINR-PA-VAT algorithm.

(b) MP-PA-VAT algorithm with $\mu = \nu = 0.1$.

Fig. 4: Optimized transmission powers ρ_i^* for: (a) Max-SINR-PA-VAT Algorithm and (b) MP-PA-VAT Algorithm with $\mu = \nu = 0.1$. Optimized for: GUEs only (green triangles, $r = 1$), UAVs only (blue circles, $r = 0$), and both GUEs and UAVs (red crosses, $r = 0.5$).

boosting the RSS at UAVs (red dash-dash line) compared to the baseline (green dash-dash line) and approaching the upper bound (blue dash-dash line), and (ii) nearly preserving the RSS at ground users (red solid line) compared to the upper bound (green solid line). Specifically, the average RSS gain at UAVs amounts to $12\,\mathrm{dB}$ and comes at the expense of an average loss of only $0.7\,\mathrm{dB}$ at ground users.

Similarly, Fig. **??** shows the CDF of the SINR perceived by ground users and UAVs when antenna tilts and transmit power are optimized through the MP-PA-VAT algorithm with $\mu = \nu = 0.1$, for ground users only, UAVs only, and both. Fig. **??** shows that the proposed algorithm reaches an SINR tradeoff, boosting the average SINR at UAVs by $13\,\mathrm{dB}$ while only incurring an average loss of $2\,\mathrm{dB}$ at ground users.

C. Generalization to Probabilistic Line-of-Sight Conditions

While the channel setup used for simulations in Section **??** assumed all GUEs to experience a non-line-of-sight (NLoS) condition, our framework is applicable to any given LoS and NLoS set up. Indeed, as per 3GPP channel modeling, the presence or absence of LoS conditions between a user at q and its corresponding BS only impacts the specific values of a_q and b_q for that particular user. Our framework is designed to accommodate generic values for these parameters. For instance, following the 3GPP model [?], if the user location q is in the LoS of its corresponding BS, we can take that into account by changing the values of $38.42\,\mathrm{dB}$ and 30 in Eqs. (**??**) and (**??**) to $34.02\,\mathrm{dB}$ and 22, respectively.

Throughout this section, we update the notation from a_q and b_q to $a_{q,n}$ and $b_{q,n}$, respectively, to accommodate the presence or absence of LoS conditions between the user at q and BS n. In the remainder of this section, we assume that UAVs are consistently in a LoS condition because of their elevated altitude [?]; however, the same reasoning can also be applied to user locations $q \in Q_U$. Let $\tau_{q,n}$ be a binary label taking the value of 1 if the user location q is in LoS with BS n and 0 otherwise. Then, we have:

$$a_{q,n} = \begin{cases} 34.02\ \mathrm{dB}, & \text{if } q \in Q_U, \\ 34.02\ \mathrm{dB}, & \text{if } q \in Q_G \text{ and } \tau_{q,n} = 1, \\ 38.42\ \mathrm{dB}, & \text{if } q \in Q_G \text{ and } \tau_{q,n} = 0, \end{cases} \tag{30}$$
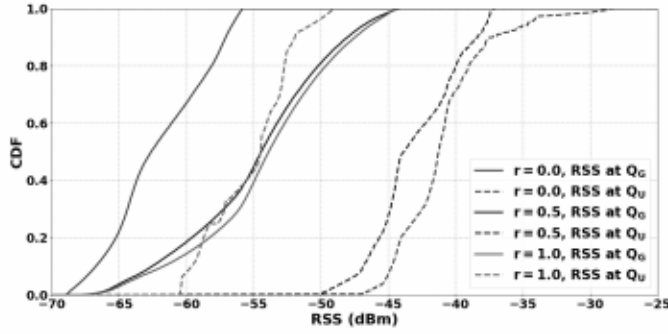
$$b_{q,n} = \begin{cases} 22, & \text{if } q \in Q_U, \\ 22, & \text{if } q \in Q_G \text{ and } \tau_{q,n} = 1, \\ 30, & \text{if } q \in Q_G \text{ and } \tau_{q,n} = 0. \end{cases} \tag{31}$$
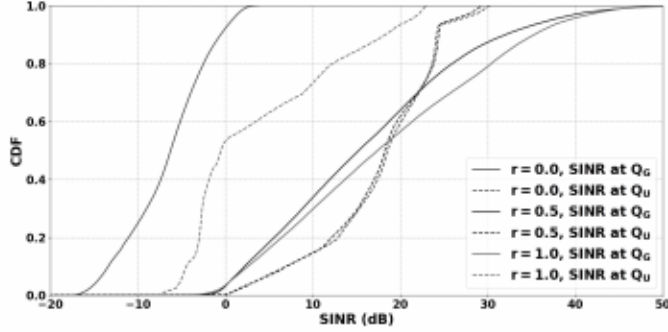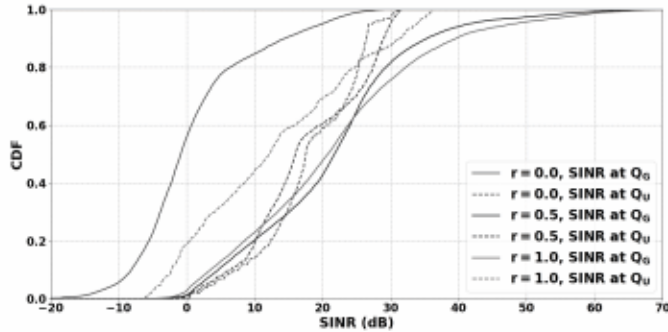
The pathloss in Eq. (**??**) is then given by:

$$L_{n,q} = a_{q,n} + b_{q,n} \log_{10} \left[\|q - p_n\|^2 + (h_q - h_{n,\mathrm{B}})^2 \right]^{\frac{1}{2}}, \tag{32}$$

while all other notations remain unaltered and all propositions still hold.

A practical case study for probabilistic LoS conditions follows from the 3GPP standard guideline in which the

(a) Max-RSS-VAT algorithm.

(b) MP-PA-VAT algorithm with $\mu = \nu = 0.1$.

(c) Max-SINR-PA-VAT algorithm under probabilistic LoS/NLoS.

Fig. 5: CDF of (a) the RSS for the Max-RSS-VAT algorithm, (b) the SINR for the MP-PA-VAT algorithm with $\mu = \nu = 0.1$, and (c) the SINR for the Max-SINR-PA-VAT algorithm under probabilistic LoS/NLoS condition. Dash-dash and solid curves represent UAVs and GUEs, respectively. Three optimization scenarios are shown: GUEs only ($r = 1$), UAVs only ($r = 0$), and both GUEs and UAVs ($r = 0.5$).

probability of LoS between the GUE at $q \in Q_G$ and BS n located at p_n is given by:

$$\mathrm{Pr}_{\mathrm{LoS}} = \begin{cases} 1, & \text{if } \|q - p_n\| \leq 18\mathrm{m}, \\ \frac{18}{\|q-p_n\|} + \left(1 - \frac{18}{\|q-p_n\|}\right)e^{-\frac{\|q-p_n\|}{63}}, & \text{otherwise.} \end{cases} \tag{33}$$

For each $q \in Q_G$ and $n \in \{1, \cdots, N\}$, the label $\tau_{q,n}$ is then created as follows: a scalar u is sampled at random from the uniform distribution $u \sim \mathcal{U}[0, 1]$. The label $\tau_{q,n}$ is set to 1 if $u \leq \mathrm{Pr}_{\mathrm{LoS}}$, and 0 otherwise. Once labels are created, the Max-SINR-PA-VAT algorithm is executed for three scenarios: $r = 0$, $r = 0.5$, and $r = 1$. Fig. **??**

illustrates the CDF of the SINR experienced by GUEs and UAVs in the three different scenarios. Similar observations as the ones in Section **??** can be made from this figure, i.e., for $r = 0.5$, there is a tradeoff between optimizing GUE and UAV performance. This tradeoff results in a substantial overall improvement in the SINR perceived by UAVs without a severe degradation in the GUE SINR. This finding showcases the broad versatility of our framework and its ability to deal with varying link conditions between users and BSs. Moreover, the algorithms could potentially extract link conditions from existing radio coverage datasets, making our algorithms well-suited for diverse real-world applications.

VI. CONCLUSION

In this paper, we took the first step towards creating a mathematical framework for optimizing antenna tilts and transmit power in cellular networks, with the goal of providing the best quality of service to both legacy ground users and UAVs flying along corridors. By applying quantization theory and designing iterative algorithms, we modeled realistic features of network deployment, antenna radiation patterns, and propagation channel models. Our proposed algorithms offer the capability to optimize coverage and signal quality while allowing for trade-offs between performance on the ground and along UAV corridors through adjustable hyperparameters. The optimal combinations of antenna tilts and transmit power, which are non-obvious and challenging to design, were shown to significantly enhance performance along UAV corridors. Importantly, these improvements come at a negligible-to-moderate sacrifice in ground user performance compared to scenarios without UAVs.

To the best of our knowledge, this is the first work that determines the necessary conditions and designs iterative algorithms to optimize cellular networks for UAV corridors using quantization theory. Our findings open avenues for further exploration and extensions from multiple standpoints, some of which are listed as follows: (i) Performance metric, optimizing for capacity per user, rather than SINR, thus aligning more closely with the objectives of real-world mobile network operators; (ii) Antenna pattern, considering BSs transmitting multiple beamformed synchronization signal blocks (SSBs), instead of a single beam, and addressing the optimization of the SSB codebooks; (iii) Cellular deployment, exploring the optimization of BS locations, in addition to their antenna tilts and transmit power; and (iv) Channel model, replacing the statistical 3GPP model with a scenario-specific map-based channel model, providing a more accurate, ad-hoc representation of the channel characteristics. Progress along any of the above directions would extend the applicability and scope of our work, paving the way for advancements in optimizing cellular networks for UAV corridors and addressing emerging challenges in air-to-ground wireless communications.